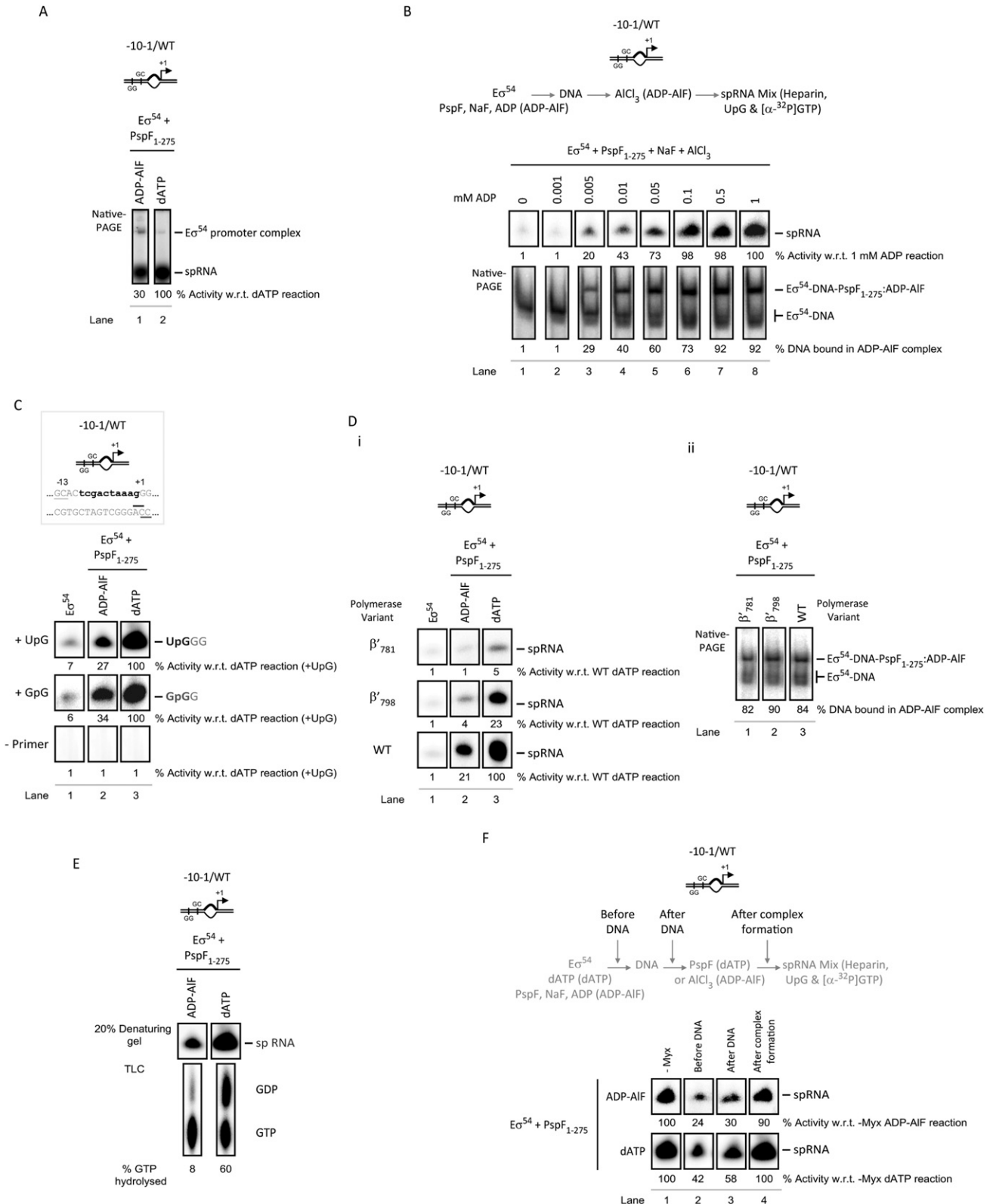
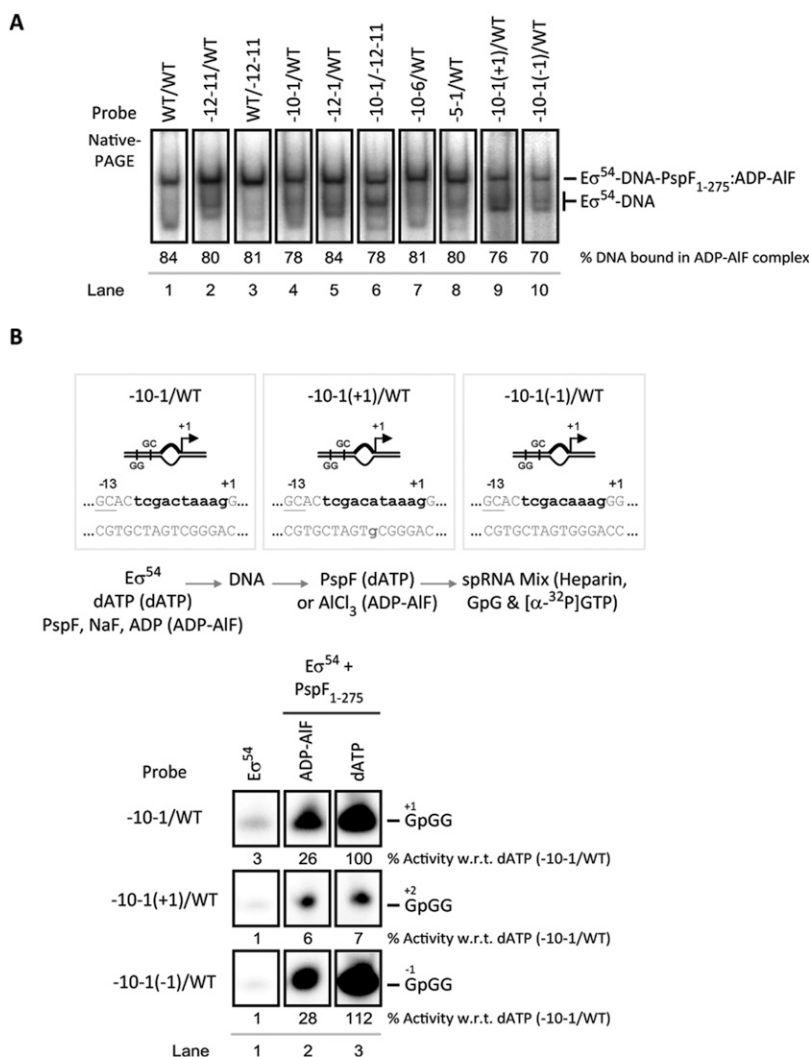


# Supporting Information

Burrows et al. 10.1073/pnas.1001188107

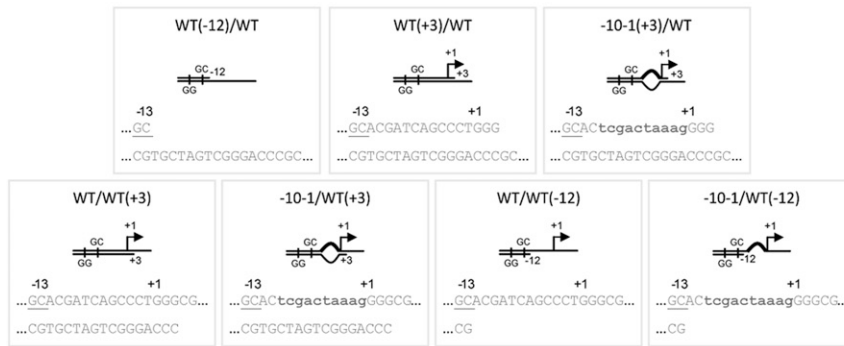


**Fig. S1.** The spRNA product supported by ADP-AIF is specific. (A) Native gel demonstrating that the spRNA product formed in the presence of either ADP-AIF or dATP is similarly released from the  $E\sigma^{54}$  promoter complex. (B) Increasing ADP concentration increases the amount of (i) ADP-AIF trapped complex [as judged by native (nondenaturing) gel analysis] and (ii) spRNA product formed. (C) Formation of the spRNA product (in both the ADP-AIF- and dATP-supported reactions) requires a specific dinucleotide primer. (Di) A catalytically active form of RNAP is required to support spRNA synthesis. (Dii) However, RNAP catalytic activity is not required for stable ADP-AIF trapped complex formation. (E) The ADP-AIF trapped form of the activator ATPase is unable to hydrolyze the GTP in the spRNA mix to form open complexes, unlike in the dATP reactions where PspF<sub>1-275</sub> is free to hydrolyze GTP (forming [ $\alpha$ -<sup>32</sup>P]GDP). (F) Myxopyronin inhibits formation of the spRNA product equally in the ADP-AIF and dATP reactions. Myxopyronin was added to the reaction mix either before DNA, after DNA addition, or after complex formation (see reaction schematic and *Materials and Methods*). In A–E, the level of spRNA synthesis has been quantified and expressed as a percentage of the amount of spRNA synthesized in the corresponding reaction (where indicated). In the native gels, the migration positions of the ADP-AIF trapped complex and  $E\sigma^{54}$ -DNA complexes are as indicated and the percentage of DNA bound in the ADP-AIF complex has been calculated and shown below the gels. The schematic representations of the probe used (where shown, the sequence has the consensus GC underlined and regions of mismatch in lowercase bold typeface) are indicated and reaction schematics (where appropriate) are shown above the gels.

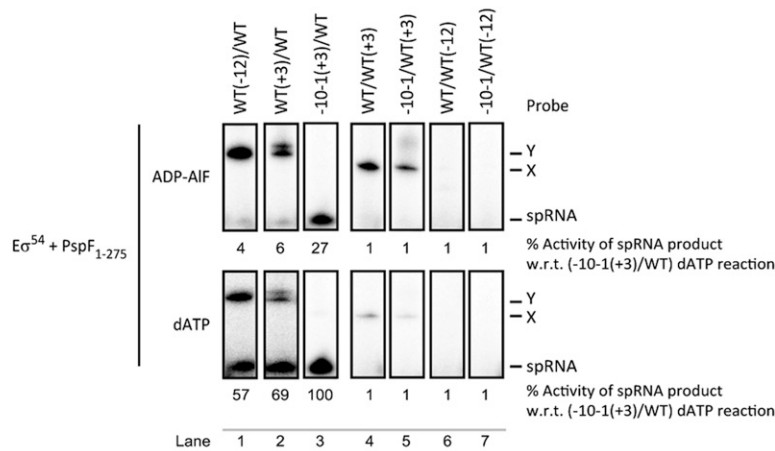


**Fig. S2.** The template requirements for spRNA synthesis. (A) Native gels illustrating that ADP-AIF complex formation was evident with all of the DNA templates tested, indicating that the lack of spRNA formation from some templates is not due to an inability to form the promoter complex. The migration positions of the ADP-AIF trapped complex and  $E\sigma^{54}$ -DNA complexes are as indicated. The percentage of DNA bound in the ADP-AIF complex has been calculated and shown below the gels. (B) The relative organization of the RNAP active site with respect to the template DNA strand in the ADP-AIF reaction is similar to that in the dATP reactions, because in both cases spRNA product synthesis can be primed from either the -1 or +1 site, but cannot be primed from the +2 site. The schematic representations of each probe (where shown, the sequence has the consensus GC underlined and regions of mismatch in lowercase bold typeface) are as indicated and reaction schematics (where appropriate) are shown above the gels. The level of spRNA synthesis has been quantified and expressed as a percentage of the amount of spRNA synthesized in the dATP (-10-1/WT) reaction (as noted).

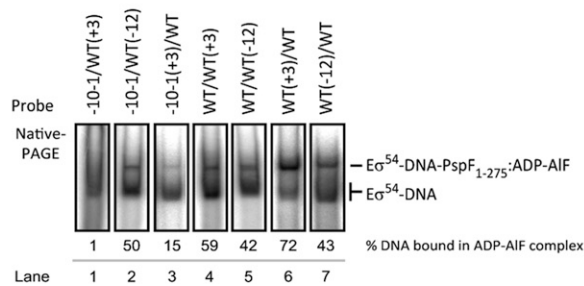
A



$E\sigma^{54}$  → DNA → PspF (dATP) → spRNA Mix (Heparin, UpG &  $[\alpha\text{-}^{32}\text{P}]\text{GTP}$ )  
 dATP (dATP) or  $\text{AlCl}_3$  (ADP-AIF)  
 PspF, NaF, ADP (ADP-AIF)



B



C

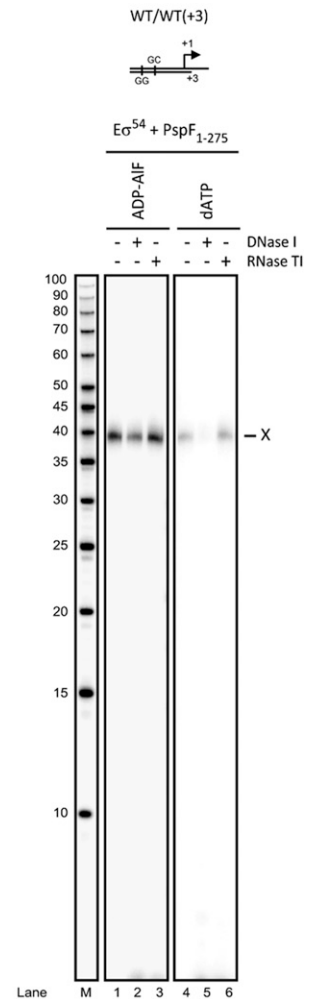


**Fig. S3.** The role of template and nontemplate DNA sequences in spRNA product synthesis. (A) Denaturing gels demonstrating that truncated templates give rise to slower-migrating species, labeled product X (in the +3 template strand truncations) and product Y (in the nontemplate strand truncations) with unusual lengths. The truncated probes used in this study have the consensus GC highlighted and regions of mismatch in lowercase bold typeface. The schematic representations of each probe are as indicated and the reaction scheme is shown above the gels. The level of spRNA synthesis was quantified and expressed as a percentage of the spRNA product synthesized in the [-10-1(+3)/WT] dATP reaction. (B) Native gels illustrating ADP-AIF complex formation in the presence of the truncated DNA templates shown in (A). The migration positions of the ADP-AIF trapped complex and  $E\sigma^{54}$ -DNA complexes are indicated. The percentage of DNA bound in the ADP-AIF complex has been calculated and shown below the gels. (C) Denaturing gels demonstrating that the +3 truncated template probe gives rise to one slower-migrating species, labeled product X, with an unusual long-length (compared with the RNA marker, lane M; USB) and very little, if any, spRNA product. Product X was sensitive to DNase I in the dATP reactions and was subsequently identified as nonspecific incorporation of  $[\alpha\text{-}^{32}\text{P}]\text{GTP}$  via extension of one DNA strand. The schematic representation of the truncated probe used in this study (with the consensus GC highlighted) is shown.

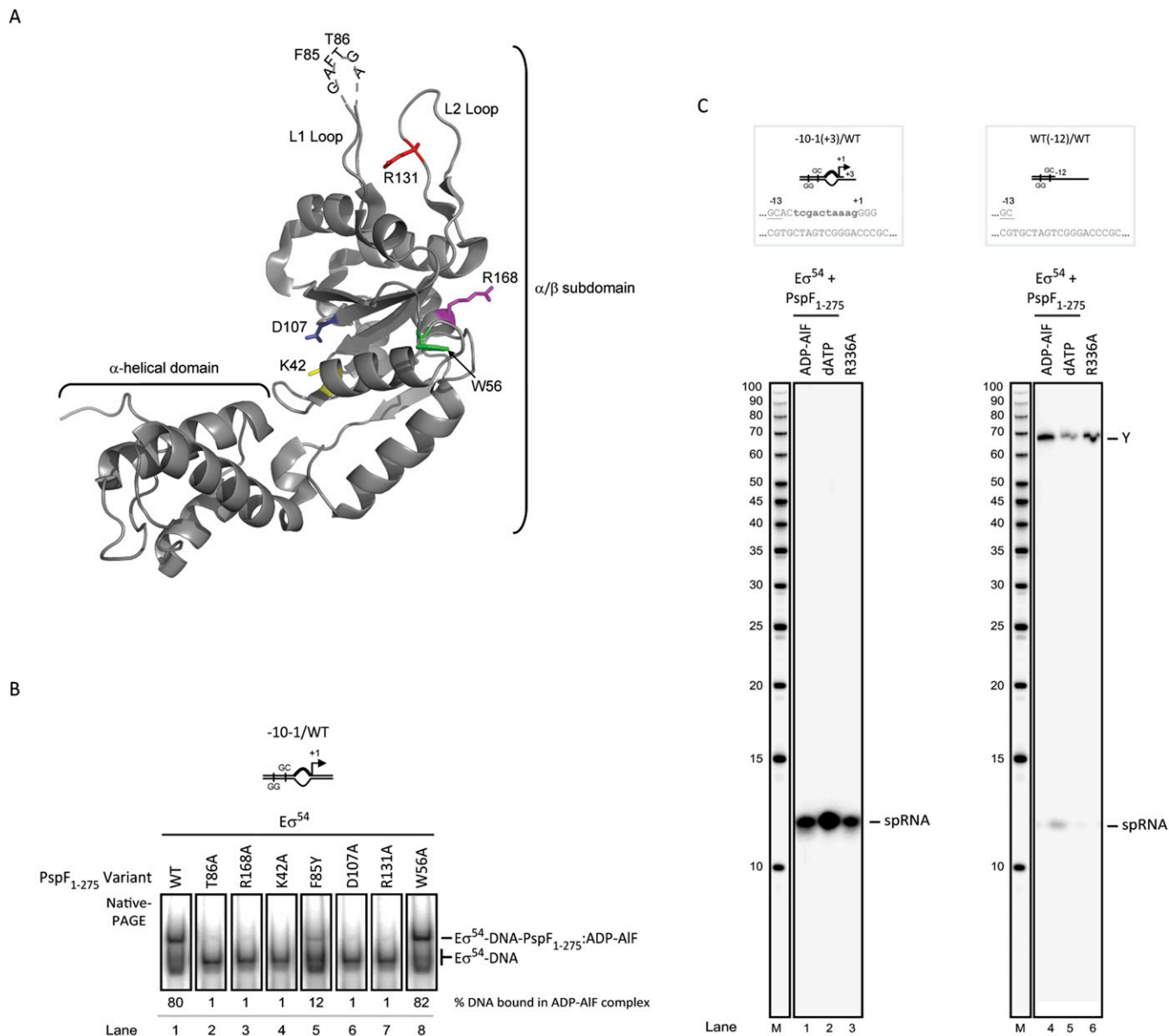


**Fig. 54.** Protein determinants required for ADP-AIF-supported spRNA synthesis. (A) The crystal structure of PspF<sub>1-275</sub> (Protein Data Bank ID code 2C9C) (1) with the L1 and L2 loop insertions, characteristic of the specialized AAA+ activator ATPases, which remodel  $\sigma^{54}$  are indicated. We note that the L1 loop is disordered within the crystal structure of PspF<sub>1-275</sub>, and as such we have inferred its structure and organization, including the site of the  $\sigma^{54}$ -interacting GAFTGA motif. The positions of residues implicated in ATP binding and hydrolysis (Walker A) K42 (yellow) and (Walker B) D107 (blue), in negative regulation W56 (which importantly has no impact on the ATPase or  $\sigma^{54}$ -interacting activities of PspF; green), intersubunit ATP hydrolysis (R-finger) residue R168 (purple), and  $\sigma^{54}$  interactions T86, F85 (inferred positions labeled T86 and F85), and indirectly (via the inappropriate presentation of the L1 loop:  $\sigma^{54}$ -interacting motif) R131 (red) are indicated. (B) Native gels illustrating the contribution of these residues to ADP-AIF complex formation. The migration positions of the ADP-AIF trapped complex and  $E\sigma^{54}$ -DNA complexes are indicated. The percentage of DNA bound in the ADP-AIF complex has been calculated and shown below the gels. (C) Denaturing gels demonstrating that truncating the nontemplate strand at -12 gives rise to a similar slower-migrating species, product Y in the R336A reaction (in the context of  $E\sigma^{54}$ ), as the ADP-AIF-supported reaction (compared with the RNA marker, lane M; USB). Product Y was subsequently identified as nonspecific incorporation of [ $\alpha$ -<sup>32</sup>P]GTP on one DNA strand. As a control, the R336A bypass variant was assayed on the +3 nontemplate truncation probe and formed the "normal" spRNA product identical to that of the ADP-AIF- and dATP-supported reactions. Schematic representation of the truncated probes used in this study with the consensus GC and regions of mismatch in bold are indicated.

1. Rappas M, et al. (2005) Structural insights into the activity of enhancer-binding proteins. *Science* 307:1972-1975.